INS #261

# INSTITUTE FOR NONLINEAR STUDIES



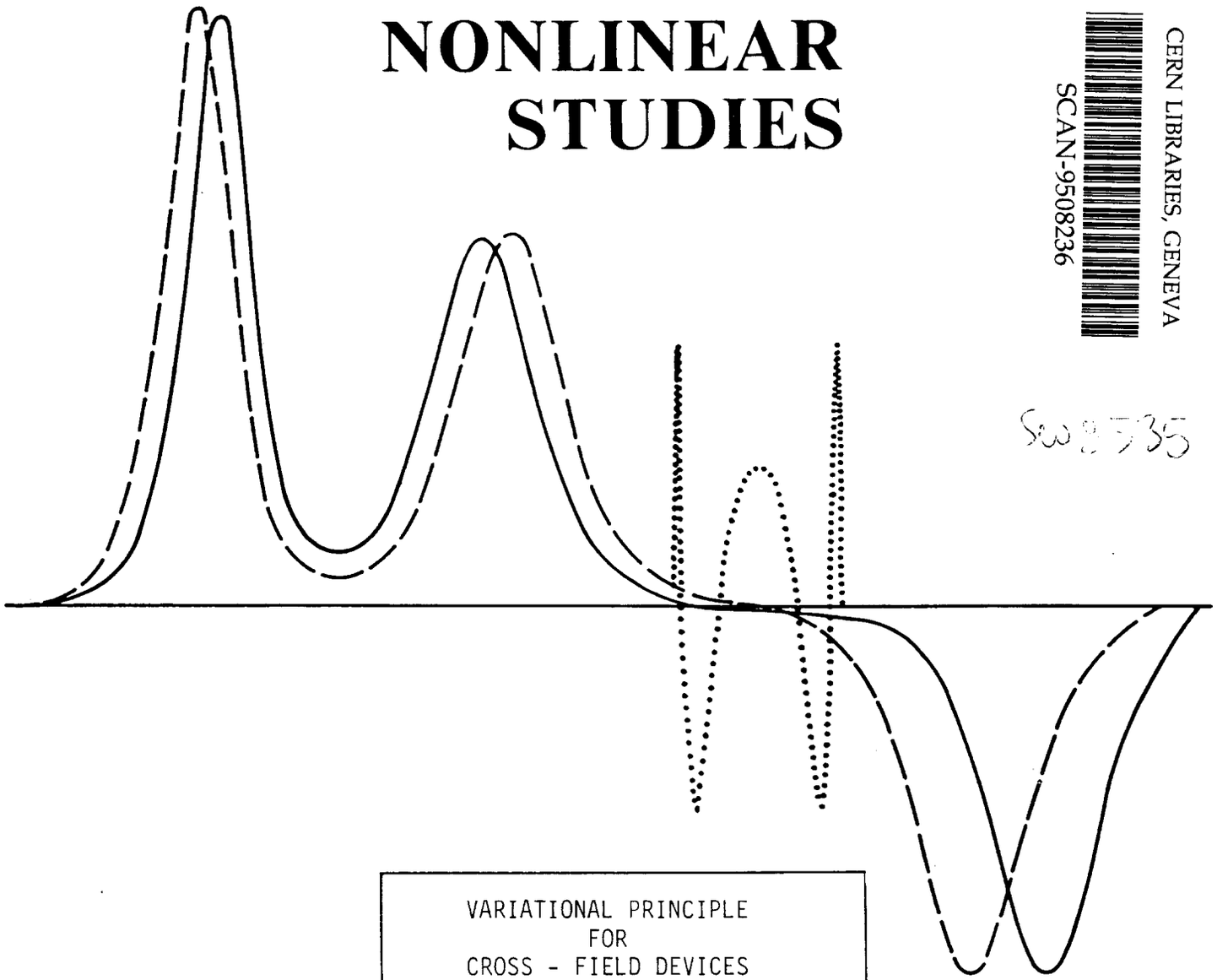

## VARIATIONAL PRINCIPLE FOR CROSS - FIELD DEVICES

by
D.J. KAUP
and
GARY E. THOMAS*

March 6, 1995

**CLARKSON UNIVERSITY**
**Potsdam, New York 13699-5815, U.S.A.**

*Varian Associates, 150 Sohier Road, Beverly, Massachusetts 01915

# Variational Principle for Cross-Field Devices

D.J. Kaup
kaup@sun.mcs.clarkson.edu
Institute for Nonlinear Studies and Department of Mathematics,
Clarkson University, Potsdam, NY 13699-5815, USA
and
Gary E. Thomas
Varian Associates, 150 Sohier Road
Beverly, Massachusetts 01915

March 6, 1995

**Abstract**

We present a variational model of the electron sheath in cross-field devices. This model not only gives an equilibrium in agreement with the classical Brillouin model, but also predicts the possible existence of nonclassical, stable equilibria with energies lower than the classical equilibrium. This model also predicts the existence of a propagating diocotron mode which is absent from the classical pure box density profile model, but is present in the double-box model. Comparisons of these results with those of the cold-fluid theory are discussed.

# 1 Introduction.

Cross-field devices are one of the major sources of high frequency $rf$ radiation as well as its amplification. Magnetrons are oscillators and cross-field amplifiers (CFA's) are high power amplifiers. The geometry of each is similar, both being cylindrical, with the major difference being that magnetrons have high aspect ratios (anode radius/ cathode radius) and few vanes while CFA's have an aspect ratio near to unity and many vanes. The significance of this difference in the mode of operation is still unclear, even in the present day. Numerical simulations of these devices can now be obtained readily and frequently do provide useful information. However they are yet to provide means for determining operating ranges for current or future devices. Thus the design of cross-field devices still remains an experimental domain.

Analytical studies have provided some useful information. Perturbation theory [1] has provided insight into the stability properties of the sheath. A double box model [2] of the sheath has provided an understanding of the initialization of operation for cross-field devices. According to the latter, once a convective cell has formed, one has a high density inner sheath and the outer adjacent lower density region of the convective cell [3]. The modulational stability of an rf wave in such a density profile has been studied [4, 1]. What one found was that the $rf$ wave is strongly modulationally unstable. Typical estimates reveal that the nonlinearity is sufficiently strong to create roughly one soliton per wavelength. Of course in this case, one no longer has a slowly varying envelope, a key simplifying assumption of the theory. However, there is still certainly some truth in this calculation since in numerical simulations, one sees a density of "spokes" on this order. This suggests that the initial formation of the spokes may well be due to a modulational instability, but with the system rapidly becoming strongly nonlinear as the spoke grows. Nevertheless, these ideas did lead to a predicted voltage operating range in much better agreement with experiment than any other theory or even numerical simulations [2].

In light of this, it would seem appropriate to try another analytical approach which could be workable for strongly nonlinear systems. Such a method is the variational principle with suitable chosen trial functions. Of course, the latter are the key to the success or failure of the method. The results will only be as good as the trial functions are close to the actual solutions. We find that a rather simple choice based on a laminar flow provides some quite interesting results. First, the model very closely approximates the classical Brillouin theory and also contains the classical Brillouin density background solution. However, there are other possible background solutions contained in this model. Among these are some that are in other regions of parameter space,

regions in which the device might not operate as expected or possibly not operate at all. Indeed, these regions may explain a missing pulse phenomenon occasionally seen the laboratory. Even though the dc voltage, dc magnetic field, and driver signal are present, sometimes a CFA does not start, i.e., it misses a pulse. However, the CFA successfully amplifies the very next driver pulse. An explanation based on the deficiency of electrons during the interpulse period has a major difficulty. How could there be enough electrons to start the tube after a pulse is missed when there weren't a sufficient number of electrons to start the missed pulse? The existence of other stable equilibria remedies this difficulty. If some background density other than the typical one was occasionally formed, then the CFA may not amplify a pulse. But this pulse would have perturbed that equilibria, probably allowing the standard equilibria to quickly re-establish itself. Then since the full space charge is still established, there are enough electrons stored to respond to the next pulse.

Second, the linearized $rf$ dispersion curves have two main branches; an acoustic-like or diocotron branch and two cyclotron branches. The surprising thing is the existence of the almost dispersion-free diocotron branch. This mode does not exist in the cold-fluid theory as a free mode. However, it appears here as a major mode. It is the assumed existance of this mode which is a key assumption in the design of a CFA. An important question is why does it appear here and why does it not appear as a free mode in the cold-fluid theory. These questions will be addressed in the concluding remarks.

In the next section, we will detail the trial functions to be used and for obtaining the initial Lagrangian. Then in Section 3, we will discuss the background solution and in Section 4, the linearized $rf$ solution. Concluding remarks will be made in the last section.

# 2 Trial Functions for a Laminar Flow.

Consider a planar configuration where the cathode is located at $y = 0$, and the anode at $y = l$, both parallel to the $xz$-plane (see Fig. 1). Let the magnetic field be in the negative $z$-direction, $\vec{B} = -B_0\hat{z}$. Let there be a positive voltage, $V$ applied to the anode with the cathode at ground potential, with an electron sheath being formed above the cathode. We shall only consider particle motion in the $xy$-plane where there is no dependence on the $z$-coordinate. Also we will use the electrostatic approximation, ignoring any $rf$ magnetic field. Under these conditions the total Lagrangian is simply

$$L = \sum_i \left[\frac{1}{2}mv_i^2 - m\Omega y_i v_{xi} + e\phi(x_i, y_i)\right]$$

$$+ \frac{1}{8\pi}\int dx \int dy[(\partial_x\phi)^2 + (\partial_y\phi)^2] \tag{1}$$

where $\phi$ is the electrostatic potential, $\Omega = eB_0/(mc)$ is the electron cyclotron frequency, $m(e)$ is the electronic mass (absolute electronic charge), $(x_i, y_i)$ are the spatial coordinates of the $i$th electron and $(v_{xi}, v_{yi})$ are its velocity components. Varying the particle's position in (1) gives the momentum equations and varying $\phi(\vec{x})$ gives Poisson's equation.

Now we shall choose trial functions for the particle orbits and the electrostatic potential. We take the particle orbits to be in laminar layers. Inside each layer, the particles move independent of the particles in the other layers (except for effects through the electrostatic potential) and oscillate about a guiding center. Let the particle positions be specified by

$$x_i = \xi_{xi} + a_0 + a_1\xi_{yi} + e_1 y_i \sin\theta_x \tag{2a}$$

$$y_i = b_1(\xi_{yi} - b_0) - f_1 y_i \cos\theta_y \tag{2b}$$

where $(\xi_{xi}, \xi_{yi})$ is the initial position of the $i$th electron, and $a_0, a_1, b_0, b_1, e_1$ and $f_1$ are arbitrary functions of time. The phases are

$$\theta_x = kx_i - \omega t + \mu \tag{3a}$$

$$\theta_y = kx_i - \omega t + \nu \tag{3b}$$

where $k(\omega)$ is the wave vector (frequency) of an $rf$ wave and $\mu$ and $\nu$ are time-dependent phase shifts. A discussion of (2) is now in order.

The first term in (2a) represents the initial $x$-position of the particle. The second term, $a_0(t)$, allows all particles, regardless of their $y$-positions, to be uniformly displaced. The third term, $\xi_{yi}a_1(t)$, allows a shear flow to be present where the $x$-component of the velocity of the particles will be proportional to $\frac{da_1(t)}{dt}$ and $\xi_{yi}$. Thus particles with larger values of $\xi_{yi}$ will move faster. The last term, $e_1 y_i \cos\theta_x$ allows the $x$-position to oscillate, with an amplitude proportional to the current $y$-position.

In (2b), the term $b_1(t)$ allows the vertical density of orbits to change. As $b_1(t)$ increases, layers move apart while if $b_1(t)$ decreases, they move closer together, giving a higher density. Initially, we take $b_1(0) = 1$ and $b_0(0) = 0$ so that $\xi_{yi}$ can be interpreted as the initial $y$-position. The factor $b_0(t)$ allows all layers to move uniformly up or down.

For any layer where $\xi_{yi} < b_0(t)$, these particle layers are inside the cathode (which is at $y = 0$) and will be excluded from the sum in (1). But if at some time later, $b_0(t)$ becomes less than $\xi_{yi}$, then that layer will have been "emitted" from the cathode and has entered the physical region. Then this layer will be counted in (1). Thus the term $b_0(t)$ allows particles to enter or leave the physical region via the cathode. The last term, $f_1 y_i \cos\theta_y$ allows the particle layers to respond vertically to an $rf$ field.

For the electrostatic potential, we model it as follows. Inside the sheath we take

$$\phi_l(x, y) = C_1 y + C_2 y^2, \tag{4a}$$

and outside the sheath we take

$$\phi_u(x, y) = V_0 [1 + V_1 \cos\theta] - d_1(l - y), \tag{4b}$$

where

$$\theta = kx - \omega t, \tag{5}$$

and the coefficients $C_1, C_2, V_0, V_1$, and $d_1$ may be time-dependent as well as functions of $\theta$. In (4a), the $C_1$ allows an electric field to be present at the cathode which then could either draw particles out, or push particles back into the cathode, depending on its sign. The term $C_2$ gives a nonzero value to $\nabla^2\phi$, required by Poisson's equation. In (4b), $V_0$ is the $dc$ potential while $V_1$ is the relative $rf$ potential at the anode. The term $d_1(l - y)$ vanishes at the anode and represents the uniform $dc$ electric field present above the sheath. The position of the upper layer of the sheath will be determined by a maximum value of $\xi_{yi} = \xi_b$, whose corresponding maximum $y$-position will be, from (2b),

$$b = b_1(\xi_b - b_0) \tag{6}$$

which is the thickness of the sheath.

At this upper layer, we need to insure continuity of $\phi$ and $\partial_y\phi$ as given by (4a) and (4b). This will give two conditions which will determine two of the coefficients in (4) in terms of the other two. We shall find it most convenient to use these conditions to express $C_2$ and $d_1$ as functions of $C_1$, $V_0$, and $V_1$.

The last thing to specify is how the sum over $i$ in (1) is to be done. Each particle is labeled with its initial position, $(\xi_{xi}, \xi_{yi})$ at $t = 0$. We take the initial distribution of particles to be given by an initial density, $n(\xi_{xi}, \xi_{yi})$, then replace the sum by an integral over $d\xi_{xi}d\xi_{yi}$. Of course, the choice of

$n(\xi_{xi}, \xi_{yi})$ is totally arbitrary. It simply describes how the particles are initially distributed before releasing them. Then once they are released, they each are constrained to evolve along the orbits given by (2).

We shall choose $n(\xi_{xi}, \xi_{yi})$ to be independent of $\xi_{xi}$ and of a box shape for the $\xi_{yi}$ dependence. Thus we take

$$n(\xi_{xi}, \xi_{yi}) = \left\{ \begin{array}{c} n_0,\ \xi_{yi} < \xi_b \\ 0,\ \xi_{yi} > \xi_b \end{array} \right\} \tag{7}$$

where $n_0$ is the initial density in the sheath and $\xi_b$ is the value of $\xi_{yi}$ at the top-most layer of particles. Note that the actual density of the sheath will be

$$n = n_0/b_1 \tag{8}$$

since the factor $b_1$ describes how the orbits will condense or rarify. Thus (1) becomes

$$\begin{aligned} L &= \int d\xi_{xi} \int_{b_0}^{\xi_b} d\xi_{yi} n_0 \left[ \frac{1}{2} m v_i^2 - m\Omega y_i v_{xi} + e\phi_i \right] \\ &+ \frac{1}{8\pi} \int dx \int_0^l \left[ (\partial_x \phi)^2 + (\partial_y \phi)^2 \right] \end{aligned} \tag{9}$$

In the next section, we discuss the result for (9) when the $rf$ field is absent ($e_1 = 0 = f_1 = V_1$) and in Section 4, we treat the linearized version of the $rf$ fields. We also scale all parameters, letting our unit of length be $l$ (the cathode-anode spacing), the unit of time, $\Omega^{-1}$, the unit of density, $\left(\frac{m\Omega^2}{4\pi e^2}\right)$, the unit of voltage, $(l^2\Omega^2 m/e)$, and scale the Lagrangian by $(12/(m\Omega^2 l^3 n_0 L_x))$ where $L_x$ is the length of the $x$-integration. Thus in these units the classical Brillouin density is when $n = 1$ and the Hull voltage is where $V_0 = \frac{1}{2}$.

# 3 The Background Solution

A key initial test for our choice of orbits will be how well they can represent the background solution. If we freeze out the $rf$ modes ($e_1 = 0 = f_1 = V_1$), then we have a pure laminar flow, the background solution of which should be an average of the cold-fluid background solution. This is indeed the case. However, we find additional features which are not found or available in the cold-fluid equations. In the cold-fluid equations, the background density profile is always arbitrary. However, for stability [5] it is known that the density gradient must be zero or negative and that the density can never exceed the Brillouin limit, [1] which is where the electron plasma frequency equals the electron cyclotron frequency. But these facts come from higher order studies (the linear perturbation of the

cold-fluid equations) and do not come from the equations for the background solution. But here, we find that regardless of the initial configuration, providing only that all particles were originally emitted from the cathode at zero velocity, all such configurations must evolve toward the Brillouin limit of $n = 1$, which is the only fixed point of these equations. One can trace this result to the effect of the variation of $b$ which allows particles to be emitted or absorbed by the cathode, a feature which cannot be easily incorporated into the cold-fluid equations.

But we also find other interesting solutions. Sometimes, experimentally it is known that one could have a residual distribution of electrons remaining in a device after it was shut down from a previous operation. Then, upon restarting the device, one would not necessarily have the above initial configuration whereby all electrons had originated from the cathode at zero velocity. So there may be practical applications of initial configurations other than the classical Brillouin initial configuration. Our variational model does allow for a wide variety of these nonclassical initial configurations. We have not attempted a full study of these nonclassical configurations, but we have noted that some of these configurations can have some rather interesting and suggestive features. For example, we find that certain such configurations could have lower energies than the classical Brillouin configuration and also seem to be stable, at least within the limits of this model. The implications that this has is that if a device upon start-up, did end up in one of these alternate configurations, then it would certainly either operate with different characteristics or possibly not at all. Such is known to occur experimentally and these alternate configurations may be an explanation for this experimental observation.

Let us now detail the above points. Letting $e_1 = 0 = f_1 = V_1$ in (8), one can obtain

$$\begin{aligned} L &= \frac{2}{n_0 l_b^2}\left[b(1-\frac{3}{4}b)C_1^2 - 2bV_0C_1(1-\frac{3}{4}b) + 3V_0^2(1-\frac{2}{3}b)\right] \\ &+ \frac{2b^2}{b_1 l_b}\left[V_0 + 2C_1(1-\frac{3}{4}b)\right] + \frac{6b}{b_1}(\dot{b} - \frac{1}{2}\dot{b}_1\frac{b}{b_1})^2 + \frac{1}{2}b^3\frac{\dot{b}_1^2}{b_1^3} \\ &+ 2\dot{a}_1^2\frac{b^3}{b_1^3} - 6\frac{b^2}{b_1^2}\dot{a}_1\dot{a}_2 + 6\frac{b}{b_1}\dot{a}_2^2 + 2\frac{\dot{a}_1 b^3}{b_1^2} - 6\frac{b^2}{b_1}\dot{a}_2 \end{aligned} \tag{10}$$

where

$$l_b = 1 - \frac{1}{2}b \tag{11}$$

$$a_2 = a_0 + \xi_b a_1 \tag{12}$$

In the above, from (2a) we see that $\dot{a}_2$ is simply the velocity at the top of the sheath and $\dot{a}_1/b_1$ is the averaged vorticity $(\partial_y v_x)$. Since $a_2$ and $a_1$ are cyclic coordinates, their momenta are constants

of the motion. These are

$$P_{a_1} = 4\frac{b^3}{b_1^3}\dot{a}_1 - 6\frac{b^2}{b_1^2}\dot{a}_2 + 2\frac{b^3}{b_1^2} \tag{13a}$$

$$P_{a_2} = 12\frac{b}{b_1}\dot{a}_2 - 6\frac{b^2}{b_1^2}\dot{a}_1 - 6\frac{b^2}{b_1} \tag{13b}$$

Let us make two observations about (13). First, if initially there is no sheath, then $b = 0$ and both momenta vanish. Also in the case of an initial Brillouin flow, from (2a), we would take $\dot{a}_0 = 0$ and $\dot{a}_1 = b_1$, whence $\dot{a}_2 = \xi_b b_1$. Then each momenta becomes proportional to the factor $\dot{b} - \xi_b b_1 (= \dot{b}_0)$. Consequently, if no additional particles have entered or left through the cathode, then $\dot{b}_0 = 0$, (which is the initial value), and these two momenta would also vanish for an initial Brillouin flow. So we see that for the two standard initial configurations, these momenta vanish. Thus, if these two momenta take on nonzero values, then they will represent configurations different from Brillouin flow and an initially empty sheath. Furthermore, by allowing the values of these momenta to have a nonzero ensemble average, one could also represent and study thermal effects.

Let us continue. Since $C_1$ has no momenta, varying it simply gives the constraint

$$C_1 = V_0 - \frac{b}{b_1} n_0 l_b \tag{14}$$

This is Poisson's equation (averaged) for this system. $C_1$ is the electric field at the cathode and as we shall shortly see, it vanishes for most equilibrium.

Another constant of motion, when $V_0$ is time independent, is the energy function, which is

$$\begin{aligned} H &= 6\frac{b}{b_1}(\dot{b} - \frac{1}{2}b\dot{b}_1/b_1)^2 + \frac{1}{2}\frac{b^3}{b_1^3}\dot{b}_1^2 \\ &+ \frac{b_1}{2b}(\frac{b_1}{b}P_{a_1} + \frac{1}{2}P_{a_2})^2 + \frac{1}{24}\frac{b_1}{b}P_{a_2}^2 + bP_{a_2} + b_1 P_{a_1} \\ &- C_1^2\frac{2b}{n_0 l_b}(1 - \frac{3}{4}b) + C_1 V_0 \frac{4b}{l_b^2 n_0}(1 - \frac{3}{4}b) - V_0^2\frac{6}{l_b^2 n_0}(1 - \frac{2}{3}b) \\ &- V_0\frac{2b^2}{b_1 l_b} - C_1\frac{4b^2}{b_1 l_b}(1 - \frac{3}{4}b) + 2\frac{b^3}{b_1} \end{aligned} \tag{15}$$

The equation of motion for $b$ and $b_1$ are obtained upon varying $b$ and $b_1$ in (10). These are

$$\begin{aligned} 12\frac{b}{b_1}\ddot{b} &- 6\frac{b^2}{b_1^2}\ddot{b}_1 + \frac{6}{b_1}(\dot{b} - \frac{b}{b_1}\dot{b}_1)^2 - \frac{2}{n_0 l_b^3}(1-b)(V_0 - C_1)^2 \\ &- \frac{4V_0 b}{b_1 l_b^2}(1 - \frac{b}{4}) - \frac{8C_1 b}{b_1 l_b^2}(1-b)(1 - \frac{3}{8}b) \\ &+ 6\frac{b^2}{b_1} - \frac{b_1}{6b^2}(P_{a_2} + 3\frac{b_1}{b}P_{a_1})^2 + P_{a_2} = 0 \end{aligned} \tag{16}$$

$$4\frac{b^3}{b_1^3}\ddot{b}_1 - 6\frac{b^2}{b_1^2}\ddot{b} - 6\frac{b}{b_1^2}(\dot{b} - \frac{b}{b_1}\dot{b}_1)^2 + 2\frac{b^2 V_0}{b_1^2 l_b}$$
$$+4\frac{b^2 C_1}{b_1^2 l_b}(1 - \frac{3}{4}b) - 2\frac{b^3}{b_1^2} + \frac{1}{6b}(P_{a_2} + 3\frac{b_1}{b}P_{a_1})^2 + P_{a_1} = 0 \qquad (17)$$

These nonlinear equations (16) and (17) describe how the model sheath parameters will evolve under various initial conditions, with $C_1$ being given by (14). While one cannot presently exclude the possible existence of interesting limit cycles, nevertheless one would expect any evolution of these equations to eventually converge to some equilibrium solution, or a fixed point, where all time derivatives vanish (providing $V_0$ also becomes a constant value as $t \to \infty$).

Setting $\dot{b} = 0 = \dot{b}_1$ in the above and using (14) gives the possible equilibrium values for $b$ and $b_1$. These can be obtained in the parametric form

$$n_0 = b_1^{(0)}(1 - \frac{1}{2}Z_1 + \frac{1}{12}Z_2^2) \qquad (18)$$

$$V_0 = b^{(0)}(1 - \frac{1}{2}b^{(0)})\frac{n_0}{b_1^{(0)}} - \frac{1}{6}b^{(0)}Z_2(1 + \frac{1}{3}Z_2) \qquad (19)$$

where $b^{(0)}$ and $b_1^{(0)}$ are the equilibrium values of $b$ and $b_1$, and

$$Z_1 = -2\frac{b_1^{(0)^2}}{b^{(0)^3}}P_{a_1} - \frac{b_1^{(0)}}{b^{(0)^2}}P_{a_2} \qquad (20a)$$

$$Z_2 = 3\frac{b_1^{(0)^2}}{b^{(0)^3}}P_{a_1} + \frac{b_1^{(0)}}{b^{(0)^2}}P_{a_2} \qquad (20b)$$

Due to the nonlinear structure of (18) - (20), it is not clear that for a given $V_0, n_0, P_{a_1}$ and $P_{a_2}$, there will be a unique solution for the equilibrium values of $b^{(0)}$ and $b_1^{(0)}$. However in the case where $P_{a_1} = 0 = P_{a_2}$, the equilibrium solution is unique and does reduce to

$$n = n_0/b_1^{(0)} = 1 \qquad (21a)$$

$$V_0 = b^{(0)}(1 - \frac{1}{2}b^{(0)}) \qquad (21b)$$

which is just the Brillouin case, in our normalized units. In this case, regardless of the initial values of $b$, $b_1$, and $n_0$, the system would cause the cathode to either supply or absorb the electrons necessary to achieve the Brillouin density with a sheath thickness compatible with the applied voltage, $V_0$.

This configuration is linearly stable within our model because if we perturb (14), (16) and (17) about this equilibrium point, the eigenfrequencies are given by

$$1 - b^{(0)} - 2\omega^2(1 - \frac{1}{2}b^{(0)}) + \omega^4 = 0 \tag{22}$$

which has only real roots for the physical range of $0 < b^{(0)} < 1$.

Let us return to the more general case. As mentioned earlier, if before start-up, a device would happen to contain some free orbiting electrons, then one could expect $P_{a_1}$ and $P_{a_2}$ to be nonzero initially. Even if these values were small, one would obtain a different equilibrium and the new equilibrium could still be linearly stable. As an example, consider the nonclassical case where $V_0 = 0.3, Z_1 = 0.2$ and $Z_2 = 0.0$. Then by the above, $n = 0.9$ and $b^{(0)} = 0.423$. For the same voltage but $Z_1 = 0 = Z_2$, we would have instead $n = 1.0$ and $b^{(0)} = 0.368$, giving a thinner but denser sheath. A stability analysis as in (22) reveals that each of these equilibria are also linearly stable. The general result is

$$\omega^4 + \omega^2\rho + \sigma = 0 \tag{23}$$

where

$$\rho = b^{(0)}(1 - Z_1 + \frac{1}{12}Z_2^2) - 2 - \frac{1}{3}Z_2(2 + Z_1 + \frac{3}{2}Z_2) \tag{24a}$$

$$\begin{aligned}\sigma &= 1 + \frac{1}{3}Z_2(2 + Z_1 + \frac{3}{2}Z_2 - \frac{1}{144}Z_2^3) \\ &+ b^{(0)}\begin{bmatrix} -1 + \frac{1}{2}Z_1 - \frac{1}{2}Z_2 + \frac{1}{8}Z_1^2Z_2 - \frac{5}{12}Z_2^2 + \frac{1}{6}Z_1Z_2^3 \\ \\ -\frac{1}{24}Z_2^3 - \frac{1}{48}Z_1Z_2^3 - \frac{1}{36}Z_2^4 \end{bmatrix}\end{aligned} \tag{24b}$$

which for $Z_1 = 0.2,\ Z_2 = 0,\ b^{(0)} = 0.423$ gives only real roots. Evaluating the potential energy function shows that this nonclassical state is also a lower energy state. Taking the velocities to be zero in (5) and evaluating at the two different equilibria, one obtains a value of $-0.612$ for the potential energy of the classical state ($Z_1 = 0 = Z_2$) while the nonclassical state ($Z_1 = 0.2, Z_2 = 0$) has a value of $-0.636$, both at the same voltage of 0.3. Thus we have a situation where a nonclassical state has a lower energy than the classical state for the same $n_0$ and $V_0$. Consequently, if the device ever did find itself in such a nonclassical state, even if the momenta $P_{a_1}$, and $P_{a_2}$ would eventually decay to zero by some mechanism, additional energy would still be required to raise the device out of the nonclassical state and into the classical one. Thus it would be possible for a device to get "hung-up" in a nonclassical state, and possible not operate.

Now on the other hand, from (24), it is clear that this is not always the case, since for large $Z_2$, these equilibria will be unstable. Still, there is a class of available nonclassical states that are stable equilibria and are nonclassical in that $Z_1$ and $Z_2$ are nonzero. At the moment, we do not see any need for further study of these states, except to note that they do exist and that if the system ever does become localized near one of these equilibria, then it could be trapped there. This has been observed occasionally and not infrequently as follows. In the laboratory, one applies the correct magnetic field, then the correct voltage and turns on the microwave input. Sometimes no amplification occurs. The device just allows the microwave power to pass through it with any amplification. When this happens, if one then just shuts everything down and restart from scratch, usually the tube will then properly operate. We suggest that the existence of these nonclassical equilibria may explain the above experimental phenomena. If before start-up, there were residual free electrons in the device, then after start-up, $Z_1$ and $Z_2$ would not have to be zero, allowing the system to possibly slip into a nonclassical equilibrium.

# 4 RF Modes.

Let us now assume that we have a classical background equilibrium where $P_{a_1} = P_{a_2} = 0$ (and thus $Z_1 = 0 = Z_2$) and

$$V_0 = b^{(0)}(1 - \frac{1}{2}b^{(0)}) \tag{25a}$$

$$n = 1 \tag{25b}$$

$$C_1 = 0 \tag{25c}$$

Under these conditions, one can evaluate the model Lagrangian, (9) for an $rf$ wave present where ($e_1, f_1, \mu$, and $\nu$) are nonzero. This will give us four nonlinear equations of motion for $e_1, f_1, \mu$, and $\nu$. Due to their complexity, we will not present these equations here. However, the most important aspect of these equations would be their small amplitude solutions because these would govern the initial evolution of an $rf$ anode wave interacting with the plasma. The linearized form of these equations have constant coefficients, whence we may analyze them using Fourier analysis. The resulting four equations reduce to

$$C_{ee}e_1 + C_{ef}f_1 \cos\delta + C_{ev}V_1 \cos\mu = 0 \tag{26a}$$

$$C_{ff}f_1 + C_{ef}e_1 \cos\delta + C_{fv}V_1 \cos\nu = 0 \tag{26b}$$

$$e_1 \left[C_{ef}f_1 \sin\delta - C_{ev}V_1 \sin\mu\right] = 0 \tag{27a}$$

$$f_1 \left[ C_{ef} e_1 \sin\delta + C_{fv} V_1 \sin\nu \right] = 0 \tag{27b}$$

where $\delta = \nu - \mu$ and

$$C_{ee} = -2l_b\omega^2 + 3bl_b\omega k - \frac{6}{5}b^2 l_b k^2 \tag{28a}$$

$$C_{ef} = 2l_b\omega - \frac{3}{4}bk \tag{28b}$$

$$C_{ff} = -2l_b\omega^2 + 3bl_b\omega k - \frac{3}{2}b^2 l_b k^2 - \frac{3b}{2l_b}(1 - \frac{2}{3}b) \tag{29}$$

$$C_{ev} = \frac{3}{4}bl_b k^2 \tag{30}$$

$$C_{fv} = -\frac{3}{10}b^2 l_b k^2 + 3(1 - \frac{2}{3}b) \tag{31}$$

and $V_1$ is the relative *rf* voltage at the anode. When $V_1$ is zero, there is only one possible solution and that is for

$$\mu = \nu \tag{29a}$$

$$C_{ee} e_1 + C_{ef} f_1 = 0 \tag{29b}$$

$$C_{ee} C_{ff} - C_{ef}^2 = 0 \tag{29c}$$

Eq. (29c) is the dispersion relation for this mode. It is a quartic in both $\omega$ and $k$, and is

$$\begin{aligned} &4l_b^2\omega^4 - 12bl_b^2\omega^3 k + \frac{72}{5}b^2 l_b^2\omega^2 k^2 \\ &-\frac{81}{10}b^3 l_b^2\omega k^3 + \frac{9}{5}b^4 l_b^2 k^4 - 4(1-b)(1-\frac{3}{4}b)\omega^2 \\ &+3b(1-b)^2\omega k - \frac{9}{16}b^2(1 - \frac{16}{5}b + \frac{32}{15}b^2)k^2 = 0 \end{aligned} \tag{30}$$

A plot of the frequency vs. $k$ for this mode is shown in Fig. 2 for $b = 0.2$. One should note that the dispersion curve is like a strongly tilted figure-8. The ratio of the $y$ and $x$ amplitudes, $(f_1/e_1)$, is shown in Fig 3.

One should note that the typical operating regime is where $\omega \sim \frac{1}{2}$ and $k \sim 10$. Thus in applications, one is really only interested in a small region of Fig. 2. We have shown the entire range of the solution so as to emphasize that the model appears to be valid over a much wider range than needed for applications.

There are two major sectors of this dispersion curve. First, the long straight middle segment, which as a slope of approximately $\frac{1}{2}b$, corresponds to the diocotron mode where $\omega \sim \frac{1}{2}v_0 k$, where $v_0$ is the drift velocity of the top of the sheath. The particle motion for this segment is mostly a

longitudinal oscillation parallel to the cathode with a smaller component transverse to the cathode, as can be seen from Fig. 3. Thus the net motion is that of a flattened ellipse. Above and below this segment are two other segments of cyclotron-like modes, where $\omega \simeq \pm\Omega + \frac{1}{2}kv_0$. These modes have roughly equal $x-$ and $y-$amplitudes, giving a net particle motion which is essentially circular. These two branches are connected together at high $k$. The two cyclotron branches are also connected at low $k$ by means of a short segment where $\omega \simeq 0$.

It is the choice of trial functions which has affected the slope of the diocotron branch and the cyclotron branches. Since we choose the amplitudes to be proportional to $y$ [see Eq.(2)], the wave is forced to sample motion throughout the sheath, not simply on the top layer, whence the factor of $\frac{1}{2}$ and not unity. Consequently, the phase velocity of this wave is an average over all drift velocities in the sheath, not just the top layer, whence the factor of $\frac{1}{2}$ and not unity.

# 5 Concluding Remarks

These results differ in several significant ways from the cold-fluid results. First one should note that this variational principle is based on a very simplified Vlasov model, in that we vary particle orbits. In the case of the background solution, variations of the particle orbits include an extremization against vertical motions, which is analogous to first-order vertical perturbations of the cold-fluid equations. Thus it is then not at all surprising that the variational model in lowest order contains some results from the higher-order cold-fluid equations, such as an equilibrium density equal to the Brillouin limit, thereby having the profile specified.

The diocotron mode does not occur in the cold-fluid theory for a pure box density profile, although analogies of the cyclotron modes are known. However it is known that if one simply very slightly modifies the pure box profile into a "double-box" profile, then the diocotron mode suddenly appears in the cold-fluid model [2]. The reason for this is that the diocotron mode requires at least a very thin layer of electrons with a different density on top of the sheath before it can appear. For a pure box density profile with an infinite density gradient at the edge of the sheath, this is not possible. But for the double-box profile, there is a step in the density profile at the edge of the sheath which then allows the diocotron mode to exist, and it exists even when the width of the step is vanishingly small, but nonzero.

This same effect is present in this variational model. Consider the particle orbits in (2) with an $rf$ wave present. All particles have an oscillating up-and-down motion. Near the edge, there will be locations in space where some but not all of the particle orbits pass through it. Thus, although

our initial distribution was a pure box (see Eq. (17)), the succeeding $rf$ oscillations introduce a structure on the edge of the density profile containing the lower density electrons necessary for the existence of the diocotron mode.

We have demonstrated that the variational principle provides a means of studying the interactions inside cross-field devices. The simple model of particle orbits given in (2) allows one to obtain physically reasonable background solutions and also reasonable dispersion curves for the $rf$ modes. Clearly there are improvements which could be made in the model, however there are mathematical advantages to keeping the model as simple as possible. As the reader may have noted, only the simplest results have been presented here. The full expansion of the Lagrangian when $e_1 \neq 0 \neq f_1$ requires pages. Equation (10) is reasonably compact only because the $rf$ modes have been frozen out. All these equations have been obtained by the simplification of general expressions derived by MACSYMA. Consequently we have many more aspects of this general problem which could and are to be explored.

# 6 Acknowledgements

This research was supported in part by the Air Force Office of Scientific Research, under grant number F49620-93-1-0088. The analytical computations were performed with the assistance of MACSYMA, a symbolic computational software.

# References


[1] D. J. Kaup, and Gary E. Thomas, Phys. Fluids B. **4**, 8 (1992).

[2] D. J. Kaup, and Gary E. Thomas, J. Appl. Phys. **71** (12) 5725 (1992).

[3] Gary E. Thomas, W.M. Bollen, D.J. Kaup, B. Goplen and L. Ludeking, Technical Digest-International Conference on Electron Devices, Washington, D.C., 1985 (IEEEE, New York, New York, 1985) pp. 180-183.

[4] D. J. Kaup and Gary E. Thomas, Stud. Appl. Math. **81**, 7-19 (1989).

[5] R. C. Davidson and K.T. Tang, Phys. Fluids **38**, 1169 (1985).

# 7 Figure Captions

Fig. 1 - The geometry of a planar CFA.

Fig. 2 - The dispersion curve of $\omega$ vs. $k$ for the $rf$ modes when $b = 0.2$.

Fig. 3 - The ratio of the $y$- to $x-$ amplitudes vs. $k$ for the $rf$ mode shown in Figure 2.

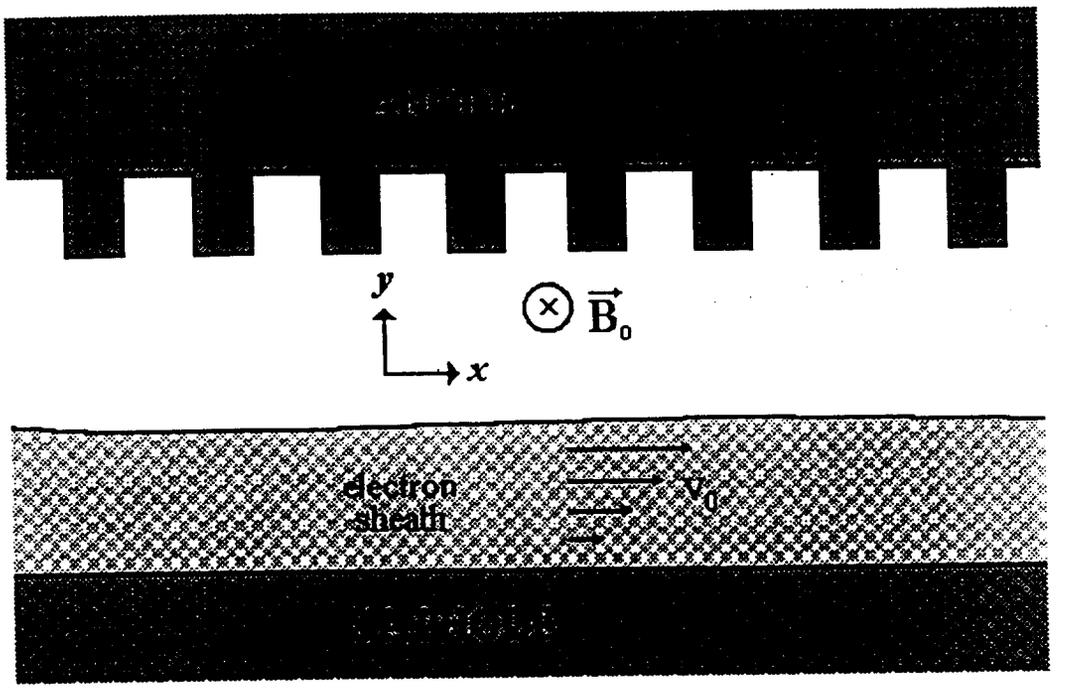


Fig. 1

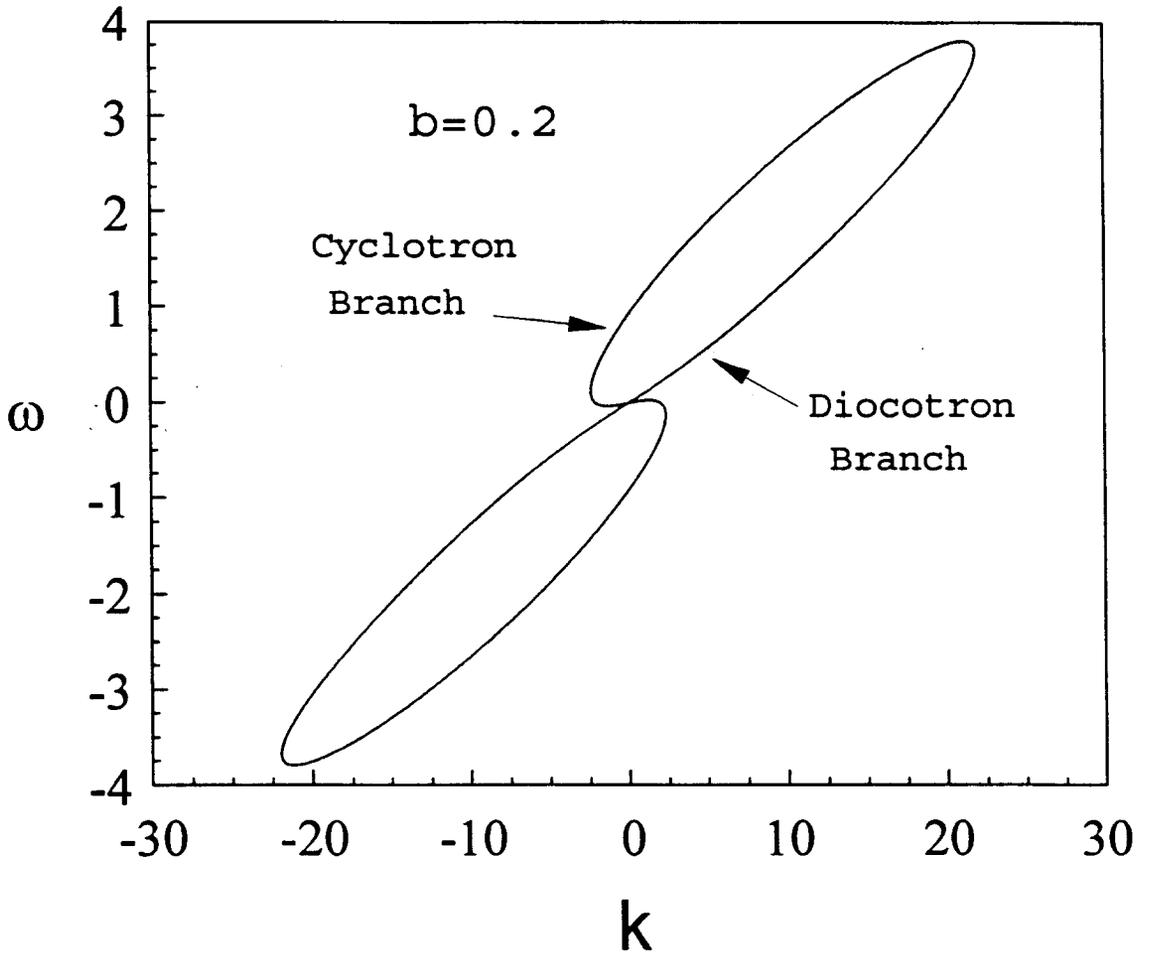
b=0.2
Cyclotron
Branch
Diocotron
Branch
ω
k
4
3
2
1
0
-1
-2
-3
-4
-30
-20
-10
0
10
20
30

Fig. 2

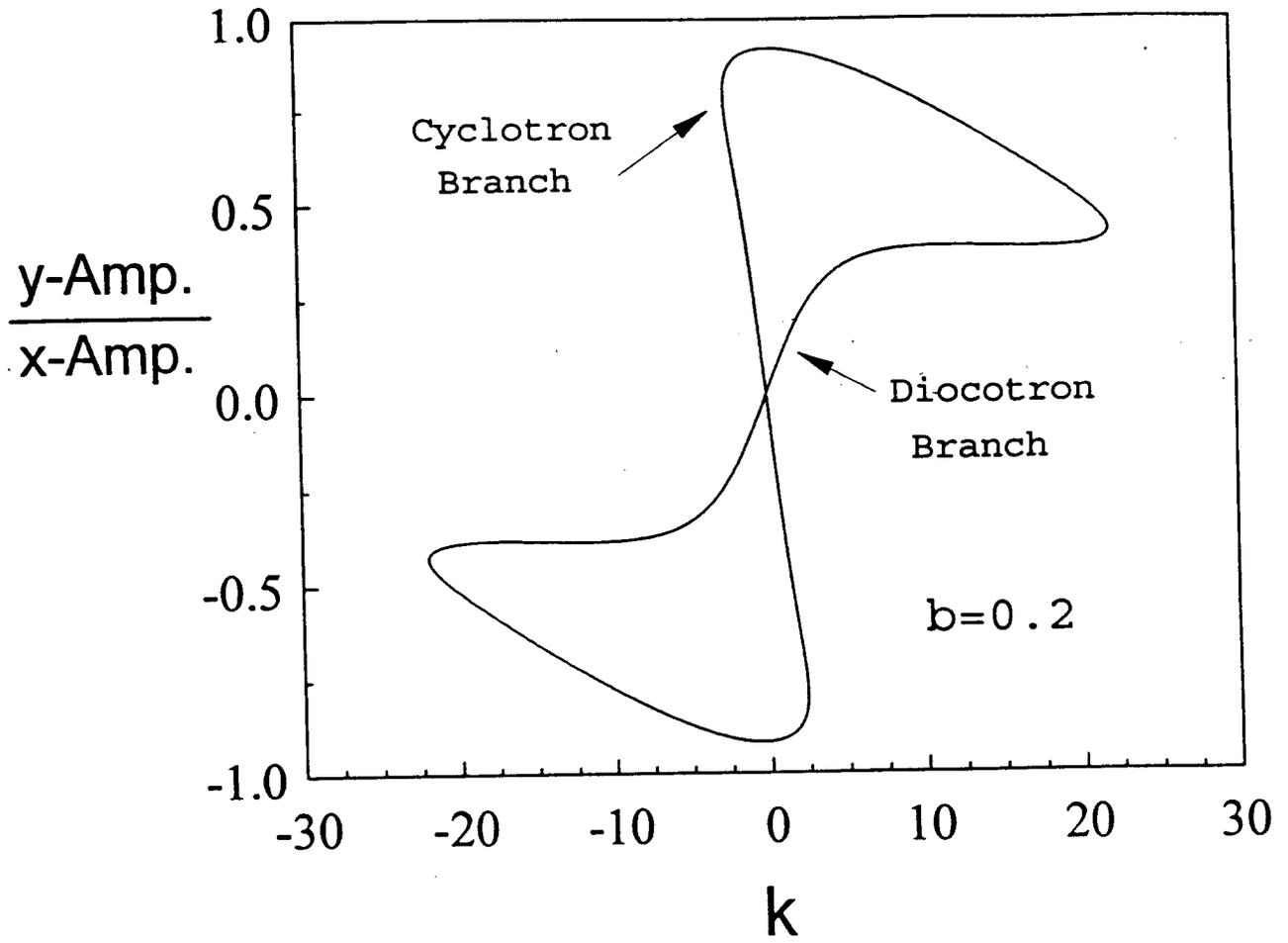
1.0
0.5
0.0
-0.5
-1.0
y-Amp.
x-Amp.
Cyclotron
Branch
Diocotron
Branch
b=0.2
-30
-20
-10
0
10
20
30
k

Fig. 3